Earthquake Engineering, Tenth World Conference © 1992 Balkema, Rotterdam. ISBN 90 5410 060 5

Seismic probabilistic reliability assessment of electric power transmission systems

A. H.-S. Ang, J. Pires, R. Villaverde & R. Schinzinger
University of California, Irvine, Calif., USA

I. Yoshida & I. Katayama
Tokyo Electric Power Services Co., Ltd, Japan

ABSTRACT: A comprehensive method for evaluating the seismic reliability of electric power transmission systems is presented. The method provides probabilistic assessments of structural damage and abnormal power flow that can lead to power interruption in a transmission system under a given earthquake. Seismic capacities of electrical equipments are determined on the basis of available test data and simple modeling from which fragility functions of specific substations are developed. Earthquake ground motions are defined as stochastic processes. Probabilities of network disconnectivity and abnormal power flow are assessed through Monte Carlo simulations. The proposed model is applied to the electric power network in San Francisco and vicinity during the 1989 Loma Prieta earthquake. This application provides a validation of the theoretical results obtained with the model.

1 INTRODUCTION

Electrical transmission equipment and facilities are vulnerable to seismic damage, particularly those in high-voltage transmission systems. Because electrical power is transmitted from the source (power plants) through various stages of voltage transformation to the consumers, failure of a high-voltage facility (e.g. substation) can cause major power blackout to a large area.

Although it is not economically feasible to totally prevent damage to a transmission system in the event of a major earthquake, quantitative (probabilistic) information on the likelihood of different levels of damage and extent of affected areas under different intensities of earthquake would be valuable for determining needed upgrading of an existing system, or for designing future systems. The same information for an existing system would be valuable also for emergency planning and disaster reduction preparedness.

A comprehensive model for the above purposes is developed and its application to the power transmission system of south San Francisco during the 1989 Loma Prieta earthquake is described. This illustrative application also serves to provide a validation of the suggested model.

2 PROBABILISTIC RELIABILITY MODEL

The proposed probability model for assessing the seismic reliability of an electrical power transmission system consists of the following components:

1. Network models for two modes of transmission failure; namely (i) failure through structural damage and disconnectivity, and (ii) failure through abnormal power flow.
2. Monte Carlo simulation procedures for calculating the probabilities of disconnectivity of a given system, and of abnormal power flow in the system.
3. Stochastic representation of site-specific seismic ground motions.
4. Determination of the seismic capacity and fragility of each type of electrical equipment, and development of fragilities of the transmission substations.

2.1 *Network connectivity model*

An electrical power transmission system consists of power generating stations, substations, supervisory control and data acquisition facilities, that are interconnected by transmission lines. The system can be modeled by a network of supply and demand nodes interconnected by links. The supply nodes represent power plants or substations which feed electric power to the demand nodes.

Disconnectivity of a demand node will occur when it is isolated from all the supply nodes. The graphical connectivity of a network model can be represented through the adjacency matrix $X = [x_{ij}]$ where,

$$x_{ij} = \begin{cases} 1, & \text{if node i is connected to node j;} \\ 0, & \text{otherwise.} \end{cases}$$

For undirected links, as in the case of electrical transmission systems, the adjacency matrix X is symmetric. The connectivity between all pairs of nodes is then determined by the connectivity or reachability matrix $C = [r_{ij}]$, which can be obtained from the adjacency matrix by standard methods (e.g., Eaton and Cohen, 1983) as,

$$C = X + X^2 + \ldots + X^n \qquad (1)$$

where,

$$r_{ij} \begin{cases} = 0, & \text{if node i is disconnected from node j;} \\ \neq 0, & \text{if node i is connected with node j.} \end{cases}$$

n = number of nodes in the network.

The connectivity matrix C is also symmetric for undirected networks. Computationally more efficient algorithms (e.g. Schinzinger, 1985) are also available for obtaining C.

Power failure at a demand node caused by disconnectivity, therefore, will occur when the demand node is totally disconnected from all the supply nodes in the network. It is possible for a power system to be split into several isolated islands. Connectivity analysis will reveal such conditions and establish the reliability of each island to continue operating autonomously.

2.2 *Power flow analysis*

Power failure or disruption at a demand node can occur also because of abnormal power flow conditions; e.g. caused by power imbalance or abnormal voltage in the transmission lines. Such conditions can be identified through a power flow analysis.

In a transmission network, it is convenient to lump the generator power and load power of a particular bus into a net bus power S_i, defined as the difference between the generator and load powers; i.e.

$$S_i = P_i + jQ_i = P_{Gi} + j(Q_{Gi} - Q_{Di}) \qquad (2)$$

The power flow equation for each bus is

$$S_i = P_i + jQ_i = V_i^* \sum_{k=1}^{n} y_{ik} V_k \qquad (3)$$

where S_i and V_i are the bus power and voltage at bus i, respectively, which are complex variables; n is the number of buses in the network system, and y_{ik} is the bus admittance. If the above power flow equation is separated into the real and imaginary parts, two equations are obtained for each bus. Of the variables P_i, Q_i, magnitude of V_i, and phase of V_i at each bus any two can be specified, such as P_i and Q_i at a load bus, or P_i and magnitude of V_i at a generating bus. Thus, for an n-bus system, the 2n unknown variables are determined from the solution of the 2n independent power flow equations. These equations are nonlinear requiring iterative methods of solution, such as the Gauss-Seidel or the Newton-Raphson method. Abnormal power flow conditions are the following:

Power Imbalance -- In a damaged transmission network, i.e., a network in which some substations and/or power stations are damaged, the total generating power may become greater or less than the total power demand. In this study, the criterion for acceptable power balance is defined by the following tolerable limits:

$$1.05 < \frac{\textit{total supply}}{\textit{total demand}} < 1.1 \qquad (4)$$

If the above condition is violated, power outage will be caused by power imbalance in the system.

Abnormal Voltage -- If the power flow analysis shows the ratio of the voltage magnitude of the damaged network, V_{damage}, to that of the base case, V_{base}, at a specific node violates a specified tolerable range, a blackout condition called abnormal voltage is reached, defined by the following,

$$\left| \frac{V_{base} - V_{damage}}{V_{base}} \right| > \alpha \qquad (5)$$

where the parameter α depends on the type of transformers in the substation (node). In this study, $\alpha = 0.2$ is used.

Unstable Condition -- Cases for which a convergent solution of the power flow equations cannot be obtained are classified as unstable conditions.

Operational Power Interruption -- A bus with abnormally high or abnormally low voltage may be causing the lack of convergence. When such a bus is removed from the network convergence is obtained. The blackout at the reference bus is an operational power interruption.

2.3 *Monte Carlo simulation*

Power failure can be caused by either disconnectivity or abnormal power flow. The respective probabilities at each demand node in the network are calculated through Monte Carlo simulations. The Monte Carlo procedure for this purpose consists of the following steps:

1. Define the base network model of the electric power transmission system.
2. Define the fragility function for each node and link in the network model, and the probability distribution of the site-specific ground motions.
3. For each simulation run (trial), failure of a component (node or link) occurs if the sampled seismic load at the component site exceeds the sampled seismic strength of the component.
4. Remove every network component that is damaged from the initial network model (base model).
5. Perform connectivity analysis and power flow analysis on the damaged network model obtained in Step 4 based on the result of the connectivity analysis; the isolated parts are removed and the network is divided into several islands if necessary. Power balance is checked and then power flow analysis is performed for each island of the damaged network model.
6. Evaluate power failure at each demand node. Two power failure modes are considered at each demand node: namely, disconnectivity from supply nodes, and abnormal power flow; each one is identified on the basis of the connectivity analysis and power flow analysis results of Step 5.
7. Repeat Steps 3 through 6 for a sufficient number of trials and evaluate the probability of power failure at each demand node as the number of trials with power failures divided by the total number of trials.

A computer program has been developed to perform the Monte Carlo simulations as outlined in the flow chart of Fig. 1.

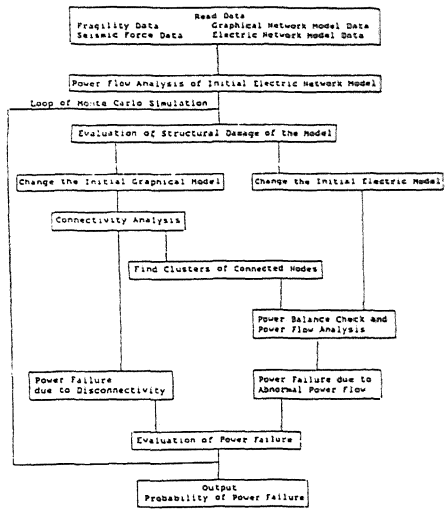

Figure 1. Flow chart of Monte Carlo simulation program

3 EARTHQUAKE GROUND MOTION MODEL

Electric power transmission systems generally cover extensive areas with some generating plants at considerable distances from the major demand sites. For reliability assessment under a given scenario earthquake, e.g., the 1989 Loma Prieta earthquake, a proper characterization of the ground motions at the various sites is needed. It is obvious, given the areal coverage of a transmission system, that ground motions at various distances from the earthquake source and for a wide variety of local site conditions are likely to be required. The maximum amplitude of the ground motions (e.g. the peak ground accelration, PGA) at a site can be deteremined through an appropriate attenuation equation. Corresponding to a given PGA, the ground motion time-history at a site can be modeled as a nonstationary random process. The proposed stochastic ground motion model defines the probability distribution, frequency content and duration of the ground acceleration at the site. In particular, a frequency and amplitude modulated filtered Gaussian white noise (Yeh and Wen, 1989) is used to represent the possible ground motion time-histories. With this model, the ground motion process is described by the instantaneous power spectral density function, S(w), intensity function, I(t), and a frequency modulation function, $\Phi(t)$. The Clough-Penzien (1973) power spectral density function is used to describe the instantaneous power spectral density function. The parameters of the model, i.e., the parameters in the analytical expressions for S(w), I(t), and $\Phi(t)$ are obtained from recorded accelerograms (Yeh and Wen, 1989).

4 SEISMIC CAPACITY AND FRAGILITY FUNCTION

Critical Equipment -- Among the different equipment in an electric transmission substation, some are critical to the proper operation of the substation and thus the fragility of a substation depends on the fragilities of these equipments.

The importance of a piece of equipment in the overall performance of a substation depends on the configuration of the substation. In many cases, a load is fed by two or more circuits and thus, the opening of one circuit does not necessarily mean interruption of power flow to that load. However, the uncontrolled opening of one redundant circuit may lead to an overload on the other circuits, which in turn would lead to the opening of the other circuits. Therefore, for all practical purposes, there is effectively no redundancy in the substations and the critical pieces of equipment in these substations are simply all those that can cause the opening of a circuit. On this basis, and the seismic equipment and structural profiles presented by Klopfenstein et al (1976) and Conway et al (1978), the equipment considered most critical are: (a) potential transformers, (b) circuit breakers, (c) current transformers, (d) coupling capacitor voltage devices (CCVD), (e) switch disconnects, and (f) bus supports. Bus supports are considered critical because if a bus support fails, the bus will most likely come in contact with the ground, a short circuit will be induced, and the associated circuit breakers will open.

4.1 *Ultimate capacity of electrical equipment*

The level of shaking that can cause the interruption of power flow at a given substation depends on the ultimate lateral capacity of each critical equipment. In general, the evaluation of the ultimate capacity involves many factors influencing the dynamic response and capacity of the equipment. Information or data on these factors are limited or difficult to define. For these reasons, the use of sophisticated analytical models to estimate the needed ultimate capacity of a critical equipment is not warranted.

In view of the above, a simple procedure is selected to estimate the required seismic capacities of the critical equipments. The dynamic properties of a given piece of equipment are first estimated from available test data and its response to a given seismic excitation is calculated by means of a simplified response spectrum approach. Additionally, simplifying assumptions include the following: (1) the equipment and its support structure are linearly elastic and respond predominantly in the fundamental mode of the combined equipment-support system; (2) the ceramic elements of the equipment are its most fragile parts and will be the first to fail under a strong earthquake; and (3) the bushings and other ceramic elements behave as cantilever beams. With these assumptions, the ultimate lateral capacity of a given piece of equipment can be determined in terms of the spectral acceleration, $SA(\omega,\xi)/g$, as:

$$R = \frac{S}{WH_{cm}}(f_t + P/A) \qquad (6)$$

where A and S are, respectively, the area and section modulus of the cross section of the ceramic element at its base; W is the weight of the equipment, H_{cm} is the distance from the base of the element to its center of mass; P is the axial force in the element induced by its own weight or a prestressing force; and f_t denotes the tensile strength of ceramic.

The ultimate capacity of a piece of equipment, therefore, basically depends on the fundamental natural frequency and damping ratio of its equipment-support system, the geometric characteristics of its ceramic elements, and the tensile strength of ceramics. As these parameters vary widely, a range of values is estimated for each of the parameters with the assumption that the values in the range are equally likely. For example, the tensile strength of ceramic insulators vary between 400 MPa and 700 MPa (Buchanan, 1986). The exception is the damping ratio -- in most of the reported tests the damping ratio is found to be close to 2 per cent.

For a given ground motion intensity, A=a, the component fragility can be defined as the probability that the spectral acceleration response, $SA(w,\xi)/g$, will exceed the lateral capacity, R, of the component. Prescribing uniform probability density functions (PDF's) for both the ultimate capacity and frequency of the equipment with the respective specified ranges of values and a constant damping ratio of 2 percent, the pertinent probability of failure is

$$P_F(A=a) = \frac{1}{(w_u - w_l)(r_u - r_l)} \int_{w_l}^{w_u} \int_{r_l}^{r_u} P[SA(\omega, 0.02)/g > r \mid A=a]\, dr\, dw \qquad (7)$$

In this study, Monte Carlo simulation is used to compute the mean and standard deviation of the spectral acceleration responses for the specified input ground motions and a Type I extreme value distribution is prescribed for $SA(\omega,\xi)/g$.

4.2 *Substation Fragility*

The substation fragility depends on the fragility of the critical pieces of equipment in the substation which, in turn, depend on the fragilities of the ceramic elements in the component. The substation fragility is obtained assuming that the fragilities for the various ceramic elements are statistically independent. Failures of only one or a few of the critical ceramic elements in a piece of equipment have been observed (Swan and Hadjian, 1988) which lends validity to this assumption.

If $R_1, R_2, \ldots, R_n$, denote the respective seismic capacities of the various critical equipments in a substation, the substation fragility is the cumulative probability distribution (CDF),

$$F_Y(y) = 1 - \prod_{j=1}^{n} [1 - F_{R_j}(y)] \qquad (8)$$

where $F_{R_j}(y)$ is the CDF of the jth equipment. As a simplification to the simulation procedure, a lognormal distribution is fitted to $F_Y(y)$ with the median, λ_Y, and coefficient of variation, ζ_Y.

5 APPLICATION TO THE LOMA PRIETA EARTHQUAKE

The electrical power transmission system in the San Francisco Bay area was heavily impacted by the Loma Prieta earthquake of 17 October 1989. The major electrical network in the affected area covering the 500 kv and 230 kv facilities in the network and the 115 kv facilities in San Francisco is shown in Fig 2. Some of the power plants and major substations experienced severe damage, and caused electric power disruption to over a million customers in the area (PG&E, 1990).

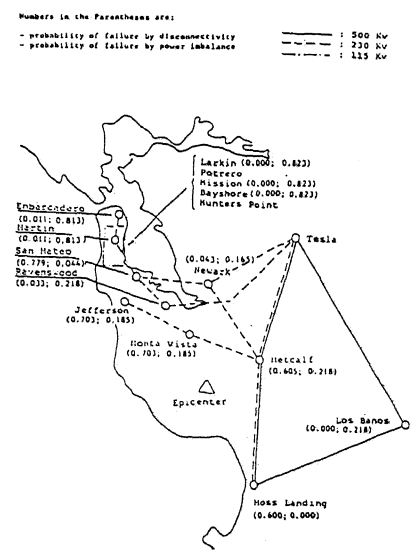

Figure 2. Bay area transmission system with respective calculated probabilities of power failures

During the Loma Prieta earthquake, ground motions were not recorded at the substations where significant damages were observed, such as the Metcalf, Monte Vista, and Moss Landing substations, which are located at distances of approximately 14 km, 21 km and 16 km, respectively, from the rupture surface. The attenuation equation developed on the basis of the Loma Prieta earthquake data is used to determine the median and C.O.V. of the peak ground accelerations (PGA) at the sites. The exception is the ground motion of the San Mateo site, a soft soil site. On this basis, the median PGA's for the above substation sites were estimated to be 0.28g, 0.22g, and 0.26g, respectively. The coefficient of variation of the PGA is 0.45 for all the sites, and the distribution of the ground acceleration is assumed to follow the lognormal distribution with the parameters given in Table 1.

Table 1. Lognormal parameters of seismic loads and fragilities

Substation or Power Plant	Load		Fragility 500 kv		Fragility 230 kv	
	λ	ζ	λ	ζ	λ	ζ
Moss Landing	-1.347	0.45	-1.336	0.1710	-1.127	0.1133
Metcalf	-1.273	0.45	-1.370	0.1170	-0.926	0.1640
Los Banos	-2.660	0.45	-1.351	0.1171		
Monte Vista	-1.514	0.45			-1.100	0.1350
Jefferson	-2.226	0.45			-1.100	0.1350
Newark	-2.230	0.45			-1.100	0.1350
Ravenswood	-1.880	0.45			-1.100	0.1350
San Mateo	-1.273	0.45			-1.609	0.1930
Martin	-2.740	0.45			-1.100	0.1350
Embarcadero	-2.740	0.45			-1.100	0.1350

Fig. 3 shows the response spectrum for one horizontal component of the Anderson dam records (downstream). The mean response spectrum for 2 percent damping obtained using the stochastic ground motion model is also shown in Fig. 3. The parameters of the ground motion model identified on the basis of the Anderson Dam records (Ang et al, 1992) are used to characterize the ground motions for the purposes of computing the substation fragilities at Metcalf, Monte Vista and Moss Landing, whereas the parameters obtained on the basis of the Foster City records are used to model the stochastic ground motion input for the San Mateo substation.

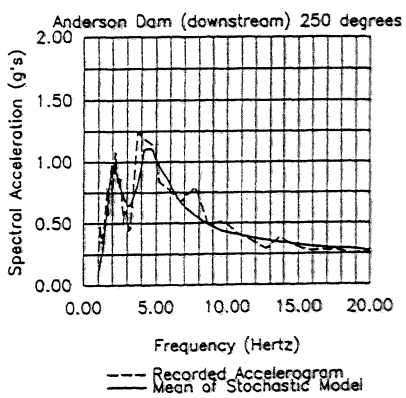

Figure 3. Response spectra of Anderson Dam record and stochastic model

Using reported experimental data, the calculated natural frequencies and ultimate lateral capacities are obtained for the critical equipment in the above substations. The values obtained for Moss Landing are presented in Table 1; similar results for the other substations are reported in Ang et al (1992). The given mean and the lower and upper values for the equipment ultimate capacities are based on an average value of 6.8 ksi for the tensile strength of ceramic reported by Buchanan (1986), a lower value of 4.26 ksi given in Electric Engineering Handbook (1976), and an upper value of 12.626 ksi, based on NGK tests of porcelain column subassemblages reported by Fischer (1991). Fragility curves for the ceramic components of selected critical equipment at the various substations are shown in Fig. 4.

Table 2. Natural frequency and capacity of electrical equipment

Equipment	Fundamental Natural Frequency (Hz)			Spectral Acceleration Causing Failure (g)		
	Lower Bound	Mean	Upper Bound	Lower Bound	Mean	Upper Bound
500-KV SWITCHYARD						
Westinghouse SF-6 live tank circuit breaker	1.5	2.0	2.5	1.37	1.91	2.66
Current transformer	1.5	2.0	2.5	1.65	2.29	3.21
Hitachi SF-6 dead tank circuit breaker	7.2	8.2	9.3	1.65	2.29	3.21
Capacitive coupling voltage transformer	2.8	3.3	3.8	1.94	2.70	3.32
Single phase step-up transformer	8.6	9.8	11.0	1.91	2.65	3.71
500/230 McGraw-Edison transformer bank	2.7	3.3	4.0	1.71	2.37	3.32
Disconnect switches	2.8	3.3	3.8	1.94	2.7	3.78
Bus support	2.8	3.3	3.8	1.94	2.70	3.78
230-KV SWITCHYARD						
Oil circuit breaker	8.6	9.8	11.0	1.91	2.65	3.71
230/115 transformer bank	8.6	9.8	11.0	1.91	2.65	3.71
Disconnect switch	1.6	2.1	2.8	2.35	3.27	4.58
Bus support	1.6	2.1	2.8	2.35	3.27	4.58

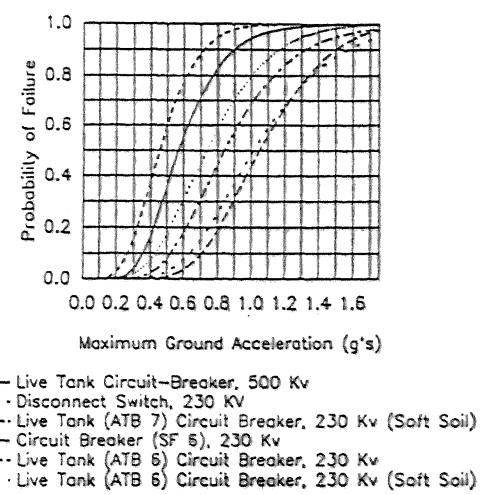

Figure 4. Fragility curves of electrical equipment.

With the assumption that seismic damage or failure of any piece of equipment in a facility (e.g. substation) will lead to the shutdown of that facility, the pertinent fragility functions for the major substations in the network were derived as summarized in Fig. 5. Each of these fragility functions can be fitted also with a corresponding lognormal distribution with the respective parameters given in Table 1.

5.1 *Disconnectivity and power flow analyses*

The performance function for a substation may be defined as

$$g(\underline{X}) = R/S \qquad (9)$$

where R = seismic capacity of the substation; and
S = maximum seismic excitation at the site.

$g(\underline{X}) \leq 1.0$, therefore, represents damage and/or power disruption of the substations.

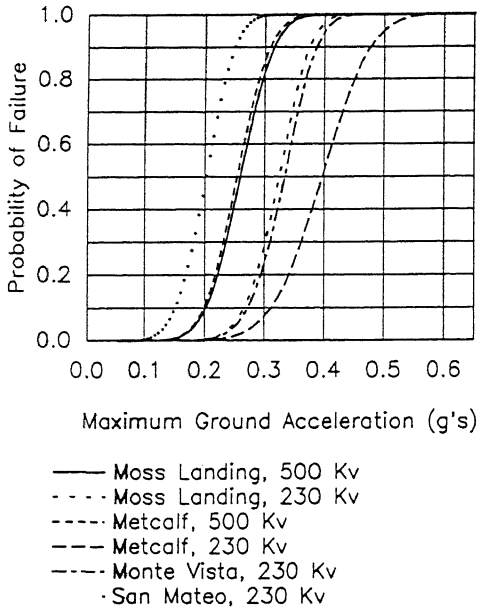

Figure 5. Fragility curves of major substations

Repeated simulations were performed for the electrical network shown in Fig. 2, using the fragility functions and site-specific ground motions for the respective substations. The damage probabilities are evaluated on the basis of Eq. 9, from which the corresponding probability of disconnectivity of each substation in the network is assessed. For each simulation, disconnectivity is realized according to the connectivity matrix of Eq. 1. The results are summarized in Table 3 and Fig. 2.

Repeated simulations were performed also for power flow of the network, from which the probability of abnormal power flow in each of the substations is evaluated. These results are also summarized in Table 3 and Fig. 2.

The Monte Carlo calculations show that power loss at the stations that were subjected to high ground accelerations, such as Moss Landing, Metcalf, Monte Vista and San Mateo, were caused largely by disconnectivity -- probabilities range from 0.600 to 0.779. In contrast, for the stations in areas of low ground accelerations, e.g. in San Francisco City, the probabilities of structural damage are small and the major contributor to power loss is power imbalance which was almost entirely caused by the blackout of the San Mateo substation.

Table 3. Calculated probabilities of power failures.

500 kv	NO.	AREA	DISCONNECTIVITY PF	DISCONNECTIVITY DEV	ABNORMAL POWER PF	ABNORMAL POWER DEV	TOTAL PF	TOTAL DEV
Los Banos	6	4	0.000	0.000	0.218	0.006	0.219	0.006
Metcalf	7	2	0.605	0.007	0.218	0.006	0.823	0.005
Tesla	8	3	0.000	0.000	0.218	0.006	0.218	0.006
230 kv								
Moss Landing	9	1	0.600	0.007	0.000	0.000	0.500	0.007
Tesla	10	3	0.000	0.000	0.218	0.006	0.218	0.006
Tesla	11	3	0.000	0.000	0.218	0.006	0.218	0.006
Metcalf	12	2	0.605	0.007	0.218	0.006	0.823	0.005
Monta Vista	13	5	0.703	0.006	0.185	0.005	0.888	0.004
Jefferson	14	6	0.703	0.006	0.185	0.005	0.888	0.004
Newark	15	7	0.000	0.000	0.218	0.006	0.219	0.006
Ravenswood	16	8	0.033	0.003	0.218	0.006	0.251	0.006
San Mateo	17	9	0.779	0.006	0.044	0.003	0.823	0.005
Martin	18	10	0.011	0.001	0.813	0.006	0.823	0.005
Embarcadero	19	11	0.011	0.001	0.813	0.006	0.823	0.005
Embarcadero	20	11	0.011	0.001	0.813	0.006	0.823	0.005
115 kv								
Martin	21	10	0.011	0.00100	0.813	0.006	0.823	0.005
San Mateo	22	9	0.779	0.00663	0.044	0.003	0.823	0.005
Larkin	23	12	0.000	0.000	0.823	0.005	0.823	0.005
Mission	24	14	0.000	0.000	0.823	0.005	0.823	0.005
Bayshore	25	15	0.000	0.000	0.823	0.005	0.823	
				0.000				

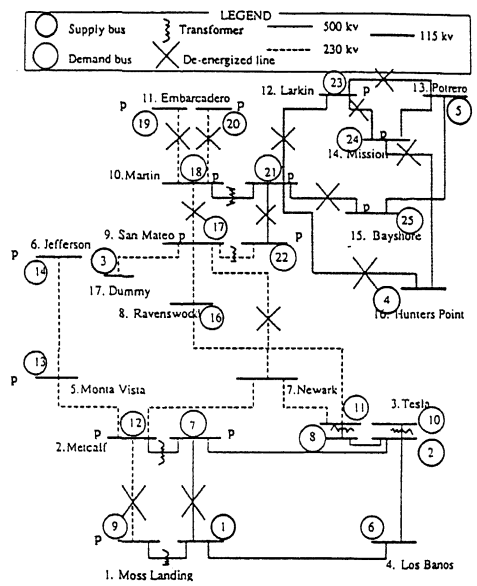

Figure 6. Blackout data (de-energized lines and station failures, p) following the earthquake.

5.2 *Comparison with blackout data*

According to post-earthquake reports (e.g. PG&E, 1990), the Moss Landing, Metcalf, and San Mateo substations were severely damaged during the Loma Prieta earthquake. The damage of the San Mateo substation severed transmission service to the San Francisco area, creating large generating/load imbalance (power imbalance) which caused a rapid frequency decline. Fig. 6 shows the actual line outages and station failures following the earthquake. This can be compared with the theoretical results of Fig. 2 obtained with the model. In particular, the theoretical results show very high failure probabilities caused by disconnectivity for those stations subjected to high-intensity ground motions. In San Francisco city, the analysis yielded high probabilities of power imbalance which are consistent also with observations following the earthquake.

6 CONCLUSIONS

Major electrical power failure during an earthquake can be caused by disconnectivity and/or abnormal power flow in a transmission network. Disconnectivity would occur primarily through structural damage of the critical equipment in the system, whereas abnormal power flow could result from power imbalance, abnormal voltage, instability, or operational power interruption. The proposed model can be used to assess the probability of either mode of failure. Implementation of the model requires stochastic definition of site-specific ground motions at the major substations, and the seismic fragility functions of the same substations.

Application of the model to the San Francisco Bay area during the Loma Prieta earthquake demonstrated the validity of the model.

7 ACKNOWLEDGEMENTS

The developments are based on a study supported primarily by the National Science Foundation under grant BCS-9011296. This support is gratefully acknowledged.

REFERENCES

Ang, A.H-S., Pires, J., Schinzinger, R., Villaverde, R. and Yoshia, I. 1992. Seismic reliability of electric power transmission systems - applications to the 1989 Loma Prieta earthquake. *Tech. Rept. to the National Science Foundation*. C.E. Dept. University of California, Irvine, CA.

Buchanan, R.C. 1986. *Ceramic materials for electronics*. Marcel Dekker, Inc.

Conway, B.J., Fong, P.T., Hawkins, G.H. and Ostrom, D.K. 1978. Seismic design guidelines for substation facilities. *IEEE Trans. on Power Apparatus and Systems* PAS-97/3: 703-713.

Clough, R. W. and Penzien, J. 1975. *Dynamics of structures*. McGraw-Hill Book Co., New York.

Electrical engineering handbook. 1976. Siemens Aktiengesellschaft. New York.

Klopfenstein, A., Conway, B.J. and Stanton, T.N. 1976. An approach to seismic evaluation of electrical substations. *IEEE Transactions on Power Apparatus and Systems* PAS-95/1: 231-242.

PG&E Co. 1990. WSCC abbreviated system disturbance report, Power Control Department.

Schinzinger, R. and Peiravi, A. 1985. "An assessment of network vulnerability. *Proc. IEEE Systems*, Man. & Cybernetics Soc. Nat. Mtg.

Shakal, A. et al. 1989. CSMIP strong motion records from the Santa Cruz mountains (Loma Prieta) earthquake of October 17, 1989. *Report OSMS 89-06*. Calif. Dept. of Conservation. Div. of Mines and Geology.

Swan, S.W. and Hadjian, A. H. 1988. The 1986 north Palm Springs earthquake: effects on power facilities. *EPRI Report No. NP-5607*.

Yeh, C. H. and Wen, Y. K. 1989. Modeling of non-stationary earthquake ground motion and biaxial and torsional response of inelastic structures. *SRS No. 546*. Univ. of Ill. at Urbana-Champaign.